# Geographic muting of changes in the Arctic sea ice cover

Ian Eisenman[1,2]

Received 23 April 2010; revised 28 May 2010; accepted 15 June 2010; published 19 August 2010.

[1] The seasonal cycle in Arctic sea ice extent is asymmetric. Its amplitude has grown in recent decades as the ice has retreated more rapidly in summer than in winter. These seasonal disparities have typically been attributed to different physical factors operating during different seasons. Here we show instead that the seasonal asymmetries in Arctic sea ice extent are a geometric consequence of the distribution of continents. Coastlines block southward ice extension during winter, thereby muting changes in ice extent, but they have relatively little effect at the time of summer minimum extent. We suggest that the latitude of the Arctic sea ice edge, averaged zonally over locations where it is free to migrate, is the most readily interpretable quantity to describe the Northern Hemisphere sea ice cover. We find that the zonal-mean sea ice edge latitude during the 1978–present era of satellite measurements has been following an approximately sinusoidal seasonal cycle that has been migrating northward at an approximately annually constant rate of 8 km/year. These results suggest a change in perspective of the most critical quantities for understanding changes in Arctic sea ice. **Citation:** Eisenman, I. (2010), Geographic muting of changes in the Arctic sea ice cover, *Geophys. Res. Lett.*, *37*, L16501, doi:10.1029/2010GL043741.

## 1. Introduction

[2] The Northern Hemisphere sea ice extent, defined as the area with a fractional sea ice cover of at least 15%, can be inferred from passive microwave satellite observations since the late 1970s. The ice extent reaches a minimum each year in September and approximately doubles by the winter maximum in March. The seasonal decay of sea ice extent is gradual during early summer and then accelerates during the remaining summer months, whereas wintertime growth is most rapid in early winter [*Parkinson et al.*, 1999; *Parkinson and Cavalieri*, 2008] (Figure 1a). A standard explanation suggests that this asymmetry between seasonal growth and decay is caused by rapid temperature changes driven by air masses from the Eurasian continent [*Peixoto and Oort*, 1992].

[3] Seasonal asymmetries in sea ice extent become more striking when rates of recent retreat are considered. Arctic sea ice retreat is typically discussed in terms of the linear trend in ice extent for each month scaled by the 1979–2000 mean extent [e.g., *Serreze et al.*, 2007]. Calculated in this manner, the sea ice extent each September has followed a downward trend of 10.9% per decade during 1979–2009, equivalent to an average loss of 34% of the perennial sea ice cover during the 31-year record. Each winter the sea ice has largely recovered the previous year's extent, albeit with a thinner ice cover [*Maslanik et al.*, 2007; *Rothrock et al.*, 2008], and the downward trend in March sea ice extent during the same period is only 2.9% per decade (Figures 1b and 1c). The year-to-year variability around the linear trend (Figure 1d) is also largest in September, such that the retreat is relatively constant throughout the year when expressed in units of detrended standard deviation [*Meier et al.*, 2007].

[4] This difference between September and March rates of retreat has often been explained in terms of a thin winter ice cover reforming where temperatures are below freezing, only to be quickly lost during the following summer melt season [e.g., *Meier et al.*, 2005]. Furthermore, trends in different elements of the climate system have been suggested to dominate the rate of ice retreat during different seasons. The gradual retreat of March sea ice extent has been attributed to changes in wind patterns and surface temperature [*Comiso*, 2006; *Francis and Hunter*, 2007; *Nghiem et al.*, 2007], whereas September ice retreat has been suggested to be driven predominantly by anomalies in downward longwave radiation fluxes [*Francis and Hunter*, 2006], with other dynamic and thermodynamic factors also contributing [*Stroeve et al.*, 2005; *Serreze et al.*, 2003; *Rigor and Wallace*, 2004; *Ogi et al.*, 2010]. However, unraveling the causal connection between wintertime air temperatures and sea ice cover is difficult because the ice cover strongly influences surface air temperature by impeding air-sea heat fluxes.

[5] Arctic sea ice extent reached a record low in September 2007, when the ice extent was 40% below the mean 1979–2000 September value (lowest red point in Figure 1e). The September 2007 sea ice low has been attributed to an unusual concurrence of events [*Perovich and Richter-Menge*, 2009]. The ice cover had thinned and was susceptible to rapid loss [*Nghiem et al.*, 2007; *Maslanik et al.*, 2007; *Kwok*, 2007], an unusual pattern of atmospheric circulation persisted through the summer with strong southerly winds advecting warm temperatures [*Comiso et al.*, 2008; *Stroeve et al.*, 2008], and a strengthened wind-driven transpolar drift caused large amounts of ice to either exit the Arctic Ocean through Fram Strait or pile up at the edge of the basin [*Zhang et al.*, 2008; *Kwok*, 2008]. Although this explanation is physically consistent, it hinges on a confluence of factors that are not obviously related.

[6] Here we focus on four central features of the observed Arctic sea ice extent evolution: *(i)* the asymmetry between seasonal growth and decay (Figure 1a), *(ii)* the seasonal disparity in the rate of recent retreat (Figure 1c), *(iii)* the seasonal differences in year-to-year variability about the

[1]Geological and Planetary Sciences, California Institute of Technology, Pasadena, CA.
[2]Department of Atmospheric Sciences, University of Washington, Seattle, Washington.


0094-8276/10/2010GL043741

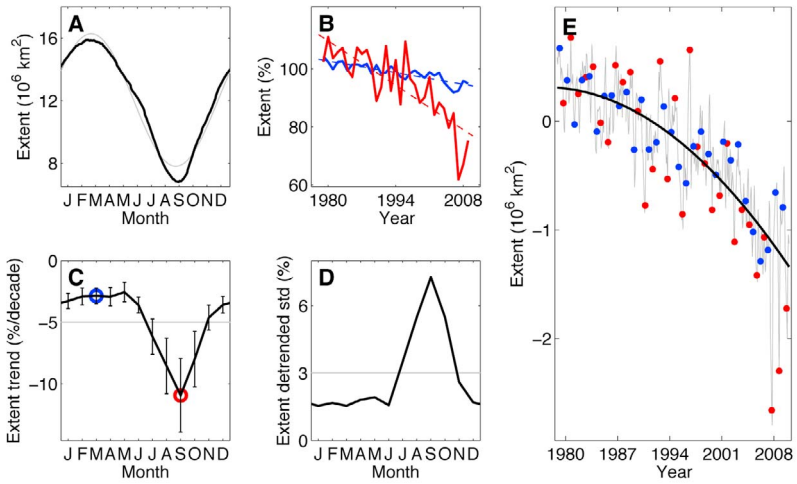


**Figure 1.** Evolution of Arctic sea ice extent (i.e., area with at least 15% sea ice cover), which is commonly used to assess sea ice changes. (a) Mean seasonal cycle during 1979–2000 (black line) with a sinusoidal fit (gray line; see auxiliary material) to emphasize the asymmetry between growth and decay. (b) Evolution of September (red) and March (blue) ice extent (solid lines), also including linear trends (dashed lines). (c) Linear trends for each month during 10/1978–1/2010, with rates at the time of winter maximum and summer minimum ice extent indicated by blue and red circles, respectively, and a gray horizontal line indicating the annual mean. Trend rates are computed by linear regression ignoring months with missing data, with error bars indicating estimated 95% regression confidence intervals. (d) Year-to-year standard deviation of the detrended ice extent, with a gray line indicating the annual mean. The trend and standard deviation are considerably larger in September than in any other month of the year. Following the standard convention, ice extents are expressed as percentages of the 1979–2000 mean for each month in Figures 1b–1d. (e) Ice extent monthly time series during 10/1978–1/2010 with the mean 1979–2000 seasonal cycle subtracted. The values in each March and September are indicated by blue and red circles, respectively, for reference. An optimal polynomial trend line (see auxiliary material) is included (black line) to illustrate the long-term mean changes.

long-term trend (Figure 1d), and *(iv)* the extreme outlier in September 2007 (Figure 1e).

## 2. Influence of Coastline Geometry

[7] The spatial structure of the sea ice seasonal cycle is shown in Figure 2a. In September, sea ice is confined to high northern latitudes and is largely contained within the Arctic Ocean (red shading in Figure 2a). Since the Arctic Ocean is bounded by land in most directions, during winter the sea ice cover extends to the shores and can only extend further southward in limited regions (Fram Strait, the Bering Sea, the Barents Sea, Baffin Bay, Hudson Bay, and the Sea of Okhotsk). At the time of winter maximum ice extent (blue shading in Figure 2a), coastlines have blocked the southward extension of sea ice at most longitudes. Hence when the ice edge migrates a given distance southward at the end of the winter growth season, the change in total hemispheric sea ice extent is relatively small.

[8] A cartoon of the Arctic coastline distribution is shown in Figure 2b. This schematically illustrates how geometric constraints of Arctic coastlines cause changes in the location

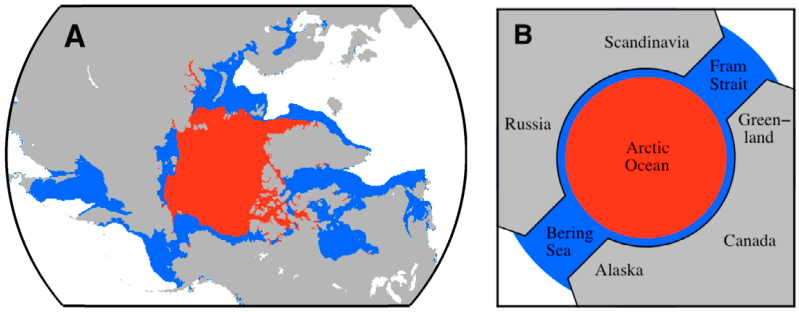


**Figure 2.** Spatial structure of sea ice seasonal cycle. (a) Mean 1979–2000 sea ice cover in September (red) and additional area covered by sea ice in March (blue). The data are plotted on a polar stereographic projection with ice-covered areas identified as grid cells which have at least 15% sea ice cover in the 22-year averages for March or September. (b) Cartoon of the Arctic coastlines illustrating how geometric constraints cause displacements of the sea ice edge near the winter maximum (blue) to have a muted effect on areal extent, in contrast to ice edge displacements near the summer minimum (red).

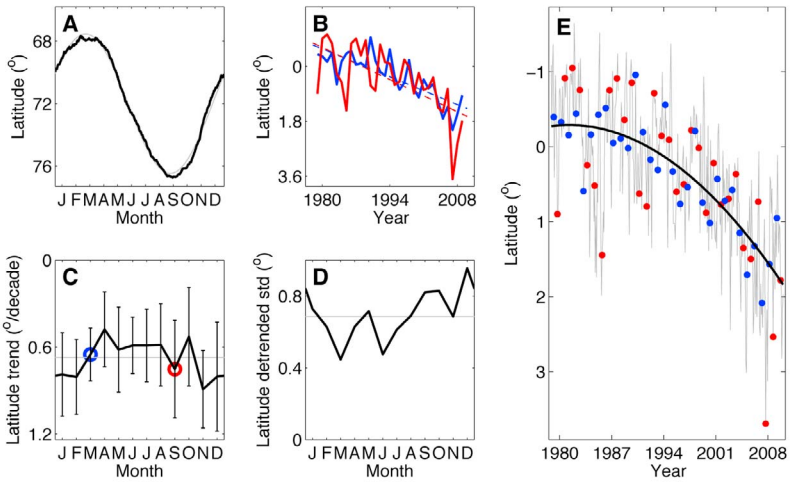


**Figure 3.** Evolution of the zonal-mean latitude of the sea ice edge, which is proposed here as a more readily interpretable quantity than ice extent. (a–e) As in Figures 1a–1e. The seasonal asymmetries in ice extent (Figure 1) disappear when changes are viewed from the perspective of ice edge latitude.

of the March ice edge to have relatively little effect on the areal extent compared with changes in the location of the ice edge in September.

[9] To quantify this effect, we examine changes in the location of the sea ice edge in satellite-derived observations of the Northern Hemisphere sea ice cover [*Cavalieri et al.*, 1996; *Meier et al.*, 2006; *Maslanik and Stroeve*, 1999]. Here we summarize the calculation, which is described in detail in the auxiliary material.[1] For each day of satellite observations, we look from the North Pole meridionally in each direction and identify the ice edge as the point with ice-covered ocean to the north and ice-free ocean to the south. Some meridians do not contain such points, instead transitioning directly from ice-covered ocean to land, and we consider these longitudes to contain no information about the ice edge latitude. We calculate the zonal-mean latitude of the sea ice edge by averaging over all longitudes in which an ice edge is identified (although as usual for zonal mean, this is merely a summary statistic, which does not imply that the ice edge latitude is zonally uniform [*Bitz et al.*, 2005]). This can be visualized in Figure 2a as the mean latitude of locations where the edge of the blue or red shading does not touch the gray shading. This leads to a time series of values for the zonal-mean ice edge latitude, which can be compared with the evolution of the ice extent.

## 3. Results

[10] The seasonal cycle of the ice edge latitude is plotted in Figure 3a. In contrast with the seasonal cycle in ice extent (Figure 1a), the ice edge latitude traces out a symmetric sinusoidal oscillation during the course of the year. The phase of the seasonal cycle in ice edge latitude (Figure 3a) demonstrates a rate of change approximately proportional to Northern Hemisphere insolation, with the ice edge latitude lagging behind insolation by 2.5 months. The central difference between Figure 1a and Figure 3a is that the ice edge latitude varies smoothly, whereas changes in ice extent are muted during winter when the ice cover is largely bounded by land. This demonstrates how geometric constraints from Arctic coastlines introduce seasonal asymmetry into the evolution of Arctic sea ice extent, despite seasonally symmetric changes in ice edge latitude.

[11] Next, we examine the rate of recent sea ice retreat. In contrast with the ice extent which retreats far more rapidly in September than in March (Figure 1b), we find that the ice edge latitude retreats at nearly identical rates in the two months (Figure 3b). In Figure 3c, the 1978–2010 trend in the ice edge latitude is plotted. For each month, the estimated 95% confidence interval (error bars) includes the annual-mean trend (gray line), demonstrating that observations are consistent with the ice edge retreating at an annually constant rate in regions where it is not blocked by land. The annual-mean trend is 8 km/year, implying an average northward displacement of 250 km during the 31-year record.

[12] The ice edge latitude year-to-year variability about the linear trend is also approximately uniform throughout the year (Figure 3d), in contrast with the ice extent which displays far larger variability during late summer than during the rest of the year (Figure 1d). Hence the seasonal cycle, rates of retreat, and detrended variability are all seasonally symmetric when viewed from the perspective of ice edge latitude.

[13] The ice edge latitude can be directly compared with ice extent by defining the "equivalent extent" as the total surface area, including land, north of the zonal-mean ice edge latitude. The equivalent extent is hence proportional to the sine of the ice edge latitude (see auxiliary material). The extent and equivalent extent are approximately equal in September but differ considerably during the rest of the year when geographic muting due to the ice cover evolution being blocked by coastlines becomes large (Figure 4).

[14] Because it evolves in an annually uniform manner, the ice edge latitude derived here provides a consistent year-round view of the evolution of the Arctic sea ice cover. Ice

[1] Auxiliary material data sets are available at ftp://ftp.agu.org/apend/gl/2010gl043741. Other auxiliary material files are in the HTML.

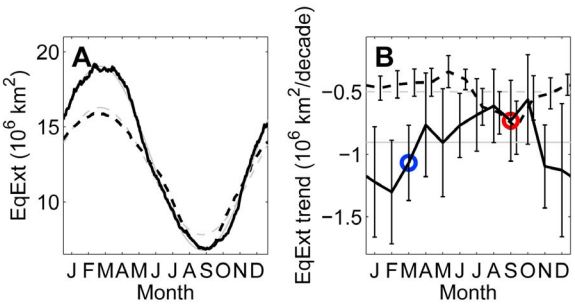


**Figure 4.** Evolution of the equivalent extent, defined as the total surface area, including land, north of the zonal-mean sea ice edge latitude. (a) Mean seasonal cycle as in Figure 1a. (b) Linear trends for each month as in Figure 1c. The ice extent is included as dashed black and gray lines for comparison in each panel; note that it is shifted slightly to the right in panel B to differentiate the error bars. In both Figures 4a and 4b, the equivalent extent is similar to the extent near the time of annual minimum (September), but the two quantities differ considerably near the time of annual maximum (March). Because the equivalent extent weighs ice edge deviations around low latitudes more heavily than high latitudes, the rate of retreat for the equivalent extent (solid line in Figure 4b) shows more seasonal structure than the ice edge latitude (Figure 3c), with changes being most rapid in wintertime. The difference between September and March ice extent trends shown here (dashed black line in Figure 4b) is approximately half as large as in Figure 1c because it is not scaled by the 1979–2000 mean seasonal cycle.

edge latitude anomalies from the mean seasonal cycle are plotted in Figure 3e. Perturbations decay quickly. The decorrelation time in units of the sampling period can be approximated as $\tau = -1/\log r$, where $r$ is the lag-one autocorrelation value. Ice edge anomalies from the polynomial trend in Figure 1e have $r = 0.55$ at a lag of 1 month, implying a decorrelation time of $\tau = 1.7$ months.

[15] Viewed from this perspective, the September 2007 minimum (lowest red point in Figure 3e) is not the largest anomaly from the accelerating long-term retreat (black line), but it is the largest anomaly to occur in September (see auxiliary material), when changes in the ice edge latitude have the largest effect on ice extent. Hence it is a significant outlier when viewed from the perspective of ice extent (Figure 1e). In other words, similarly large negative ice edge anomalies have occurred previously during months when a considerable fraction of the ice edge was blocked by continents and the associated changes in ice extent were muted. This implies that the unprecedented minimum sea ice extent in September 2007 may simply be part of a noisy but annually constant retreat, with the relative change in ice extent being amplified through aliasing of the noise by the geographic effects described here. Hence such an extreme outlier in September ice extent could occur again in the future. This result may help explain why September 2007 appeared as an outlier from the perspective of ice extent while apparently lying near the trend line from the perspective of ice thickness [*Lindsay et al.*, 2009].

[16] Considering the zonal-mean ice edge latitude instead of ice extent may also be useful in the interpretation of global climate model simulations. To facilitate calculation of the ice edge latitude from ice extent, an approximate relationship is given in the auxiliary material.

## 4. Conclusions

[17] These results suggest that the seasonal asymmetries in the evolution of Arctic sea ice extent are overwhelmingly the consequence of blocking by coastlines. When viewed instead from the perspective of zonal-mean ice edge latitude, the asymmetries disappear. Hence while the ice extent is useful for describing the climate response to changes in the sea ice cover, the zonal-mean ice edge latitude proposed here may provide a more readily interpretable description of the response of sea ice to climate changes. We find that the observed ice edge latitude traces out a seasonal cycle consistent with a linear response to hemispheric insolation, and that it has been retreating in recent decades at an annually constant rate. Attention on Arctic sea ice retreat has previously been focused on the summer minimum (September), when ice extent diminishes most rapidly. Our results show that the location of the sea ice edge has been receding just as rapidly during wintertime, but that geometric effects of Arctic coastline geography have caused the retreat during much of the year to appear muted in previous analyses which have focused on ice extent.

[18] **Acknowledgments.** Many thanks to Tapio Schneider, Peter Huybers, Eli Tziperman, Norbert Untersteiner, Yohai Kaspi, Tim Merlis, Kyle Armour, John Walsh, and J. S. Wettlaufer for helpful comments. Thanks to the National Snow and Ice Data Center for providing the data used in this study and to Walt Meier for generous assistance processing it. This work was supported by NSF grant ATM-0502482, a Prize Postdoctoral Fellowship through the Caltech Division of Geological and Planetary Sciences, and a NOAA Climate and Global Change Postdoctoral Fellowship administered by the University Corporation for Atmospheric Research.

## References

Bitz, C. M., M. M. Holland, E. C. Hunke, and R. E. Moritz (2005), Maintenance of the sea-ice edge, *J. Clim.*, *18*(15), 2903–2921.

Cavalieri, D., C. Parkinson, P. Gloerson, and H. Zwally (1996), Sea ice concentrations from Nimbus-7 SMMR and DMSP SSM/I passive microwave data, 1978–2007, http://nsidc.org/data/nsidc-0051.html, Natl. Snow and Ice Data Cent., Boulder, Colo. (Updated 2008.)

Comiso, J. C. (2006), Abrupt decline in the Arctic winter sea ice cover, *Geophys. Res. Lett.*, *33*, L18504, doi:10.1029/2006GL027341.

Comiso, J. C., C. L. Parkinson, R. Gersten, and L. Stock (2008), Accelerated decline in the Arctic sea ice cover, *Geophys. Res. Lett.*, *35*, L01703, doi:10.1029/2007GL031972.

Francis, J. A., and E. Hunter (2006), New insight into the disappearing Arctic sea ice, *Eos Trans. AGU*, *87*, 509–524, doi:10.1029/2006EO460001.

Francis, J. A., and E. Hunter (2007), Drivers of declining sea ice in the Arctic winter: A tale of two seas, *Geophys. Res. Lett.*, *34*, L17503, doi:10.1029/2007GL030995.

Kwok, R. (2007), Near zero replenishment of the Arctic multiyear sea ice cover at the end of 2005 summer, *Geophys. Res. Lett.*, *34*, L05501, doi:10.1029/2006GL028737.

Kwok, R. (2008), Summer sea ice motion from the 18 ghz channel of AMSR-E and the exchange of sea ice between the Pacific and Atlantic sectors, *Geophys. Res. Lett.*, *35*, L03504, doi:10.1029/2007GL032692.

Lindsay, R. W., J. Zhang, A. Schweiger, M. Steele, and H. Stern (2009), Arctic sea ice retreat in 2007 follows thinning trend, *J. Clim.*, *22*(1), 165–176, doi:10.1175/2008JCLI2521.1.

Maslanik, J., and J. Stroeve (1999), Near real-time DMSP SSM/I daily polar gridded sea ice concentrations, January 2009–January 2010, http://nsidc.org/data/nsidc-0081.html, Natl. Snow and Ice Data Cent., Boulder, Colo. (Updated daily.)

Maslanik, J. A., C. Fowler, J. Stroeve, S. Drobot, J. Zwally, D. Yi, and W. Emery (2007), A younger, thinner Arctic ice cover: Increased potential for rapid, extensive sea-ice loss, *Geophys. Res. Lett.*, *34*, L24501, doi:10.1029/2007GL032043.

Meier, W., J. Stroeve, F. Fetterer, and K. Knowles (2005), Reductions in Arctic sea ice cover no longer limited to summer, *Eos Trans. AGU*, *86*(36), 326, doi:10.1029/2005EO360003.

Meier, W., F. Fetterer, K. Knowles, M. Savoie, and M. J. Brodzik (2006), Sea ice concentrations from Nimbus-7 SMMR and DMSP SSM/I passive microwave data, January–December 2008, http://nsidc.org/data/nsidc-0051.html, Natl. Snow and Ice Data Cent., Boulder, Colo. (Updated 2009.)

Meier, W. N., J. Stroeve, and F. Fetterer (2007), Whither Arctic sea ice? A clear signal of decline regionally, seasonally, and extending beyond the satellite record, *Ann. Glaciol.*, *46*, 428–434, doi:10.3189/172756407782871170.

Nghiem, S. V., I. G. Rigor, D. K. Perovich, P. Clemente-Colón, J. W. Weatherly, and G. Neumann (2007), Rapid reduction of Arctic perennial sea ice, *Geophys. Res. Lett.*, *34*, L19504, doi:10.1029/2007GL031138.

Ogi, M., K. Yamazaki, and J. M. Wallace (2010), Influence of winter and summer surface wind anomalies on summer Arctic sea ice extent, *Geophys. Res. Lett.*, *37*, L07701, doi:10.1029/2009GL042356.

Parkinson, C. L., and D. J. Cavalieri (2008), Arctic sea ice variability and trends, 1979–2006, *J. Geophys. Res.*, *113*, C07004, doi:10.1029/2007JC004564.

Parkinson, C. L., D. J. Cavalieri, P. Gloersen, H. J. Zwally, and J. C. Comiso (1999), Arctic sea ice extents, areas, and trends, 1978–1996, *J. Geophys. Res.*, *104*(C9), 20,837–20,856, doi:10.1029/1999JC900082.

Peixoto, J. P., and A. H. Oort (1992), *Physics of Climate*, 520 pp., Am. Inst. Phys., College Park, Md.

Perovich, D. K., and J. A. Richter-Menge (2009), Loss of sea ice in the arctic, *Ann. Rev. Mar. Sci.*, *1*, 417–441, doi:10.1146/annurev.marine.010908.163805.

Rigor, I. G., and J. M. Wallace (2004), Variations in the age of Arctic sea-ice and summer sea-ice extent, *Geophys. Res. Lett.*, *31*, L09401, doi:10.1029/2004GL019492.

Rothrock, D. A., D. B. Percival, and M. Wensnahan (2008), The decline in Arctic sea-ice thickness: Separating the spatial, annual, and interannual variability in a quarter century of submarine data, *J. Geophys. Res.*, *113*, C05003, doi:10.1029/2007JC004252.

Serreze, M. C., et al. (2003), A record minimum Arctic sea ice extent and area in 2002, *Geophys. Res. Lett.*, *30*(3), 1110, doi:10.1029/2002GL016406.

Serreze, M. C., M. M. Holland, and J. Stroeve (2007), Perspectives on the Arctic's shrinking sea-ice cover, *Science*, *315*(5818), 1533–1536, doi:10.1126/science.1139426.

Stroeve, J., M. Serreze, S. Drobot, S. Gearheard, M. M. Holland, J. Maslanik, W. Meier, and T. Scambos (2008), Arctic sea ice extent plummets in 2007, *Eos Trans. AGU*, *89*(2), 13–14, doi:10.1029/2008EO020001.

Stroeve, J. C., M. C. Serreze, F. Fetterer, T. Arbetter, W. Meier, J. Maslanik, and K. Knowles (2005), Tracking the Arctic's shrinking ice cover: Another extreme September minimum in 2004, *Geophys. Res. Lett.*, *32*, L04501, doi:10.1029/2004GL021810.

Zhang, J. L., R. Lindsay, M. Steele, and A. Schweiger (2008), What drove the dramatic retreat of Arctic sea ice during summer 2007?, *Geophys. Res. Lett.*, *35*, L11505, doi:10.1029/2008GL034005.

I. Eisenman, Geological and Planetary Sciences, California Institute of Technology, 1200 California Blvd., Pasadena, CA 91125, USA. (ian@gps.caltech.edu)

# Auxiliary Material for 2010GL043741

### Calculating the zonal-mean ice edge latitude

This study uses daily sea ice concentration (i.e., fractional sea ice cover) derived with the NASA Team algorithm from Nimbus-7 SMMR (1978–1987), DMSP SSM/I (1987–2009), and DMSP SSMIS (2008–present) satellite passive microwave radiances on a nominally 25km×25km polar stereographic grid [*Cavalieri et al.*, 1996; *Meier et al.*, 2006; *Maslanik and Stroeve*, 1999]. Lakes are masked out of the concentration fields, and the 2°–5° circular section around the North Pole which is not imaged is assumed to be ice-covered. During periods of transition from an instrument onboard one satellite to another, daily ice concentration fields from both satellites are typically available for several months, and we take an average over the two fields. Final ice concentration data is currently available from NSIDC through the end of 2007 [*Cavalieri et al.*, 1996], but only preliminary [*Meier et al.*, 2006] and near-real-time [*Maslanik and Stroeve*, 1999] concentration data is available for more recent dates. Missing pixels are present in the preliminary and near-real-time concentration fields, although they are not present in the final concentration fields because they have been filled using spatial and temporal interpolation. We fill missing pixels in the preliminary and near-real-time daily concentration fields with monthly-mean concentration values.

We calculate the ice extent and zonal-mean ice edge latitude from each daily sea ice concentration field. The extent is calculated by summing the areas of all grid boxes with at least 15% ice concentration. This is a widely used current definition of ice extent [e.g., *Parkinson and Cavalieri*, 2008], although we note that for pre-satellite data ice extent has historically been defined instead as the ocean area poleward of the 15% ice concentration contour [e.g., *Walsh*, 1995]. For the ice edge latitude, we begin by interpolating the ice concentration maps onto a uniform 0.5°×0.5° latitude–longitude grid using triangle-based linear interpolation. At each longitude, we seek adjacent grid boxes where the box to the north has ice concentration greater than 15% and the box to the south has less than 15% concentration (similar to the characterization of the ice edge in isolated longitude bands used in previous studies [*Francis and Hunter*, 2006, 2007]), and we exclude locations where either grid box is adjacent to land. If multiple latitudes satisfy these criteria for a given longitude, the northernmost location is selected. The number of zonal points satisfying these criteria varies from day to day, with the September average being 392 points and the March average being 271 points. This corresponds to 46% and 62% of the meridians being blocked by land in September and March, respectively. The exact latitude associated with 15% ice concentration at each longitude is found by linear interpolation of the ice concentration between the latitudes of the centers of the two adjacent grid boxes. Finally, we average over all longitudes where these criteria are met. This leads to daily time series of the ice extent and the zonal-mean ice edge latitude. The results presented here are not qualitatively affected if the southernmost latitude is used instead when multiple latitudes satisfy the criteria, or if locations are excluded that lie within 2 rather than 1 grid points of land.


0094-8276/10/$5.00

To avoid biases associated with the merging of temporal and spatial means in monthly-mean ice concentrations, monthly data is calculated by averaging the ice extent and zonal-mean ice edge latitude over all days in each month, rather than deriving the ice extent and ice edge latitude from monthly-mean sea ice concentration fields. Months which do not have at least 20 days of ice concentration data (10 days of data for SMMR, which operated every other day) are excluded. This occurs for three months during the record (10/1978, 12/1987, and 1/1988).

The equivalent extent is computed as $2\pi r^2(1 - \sin\phi_i)$, where $r$ is the radius of the earth and $\phi_i$ is the zonal-mean ice edge latitude.

### Sinusoidal fit and optimal polynomial trend

The sinusoidal fits in Figs. 1A, 3A, and 4A are computed by minimizing mean squared deviation. The root mean squared difference between the data (black solid lines) and the sinusoid (gray solid lines) in Figs. 1A, 3A, and 4A is 0.506, 0.263, and $0.297 \times 10^6$ km$^2$, respectively.

The order of the polynomial trend line for the data in Fig. 3e is chosen using leave-one-out cross-validation, which suggests an optimal fit by a third-order polynomial, with second-order being only slightly less optimal. This statistical method is equivalent to removing each point in the time series, one by one, and examining the error associated with estimating the removed point using a polynomial fit of the remaining data [*Weisberg*, 2005]. Because this method has a slight tendency to overestimate the polynomial order [*Shao*, 1993], we plot a second-order polynomial trend line in Fig. 3e, although a third-order polynomial trend gives a similar visual effect. We also use a second-order polynomial trend in Fig. 1e for consistency.

Extrapolation of the polynomial trend in Fig. 3E into the future implies a seasonally ice-free Arctic Ocean by year 2029–2066 and, more remarkably, an Arctic Ocean which is ice-free throughout the year starting in year 2037–2093. Specifically, a second-order polynomial fit implies seasonally ice-free conditions by year 2057 and annually ice-free conditions by year 2079. Using the standard error of prediction from future noise and errors in the multilinear regression coefficients, the estimated 95% confidence intervals are 2050–2066 and 2070–2093, respectively. A third-order polynomial fit implies seasonally and annually ice-free conditions by years 2034 (2029-2043) and 2043 (2037–2056), respectively. It should be emphasized that although such an extrapolation is illustrative of the rapidity of the rate of observed ice retreat, it is unlikely to provide a reliable prediction. The optimal fit polynomial, as well as the annually uniform nature of the retreat, can be expected to vary in the future. Credible predictions must ultimately be based on physical models, although sea ice predictions may not yet be reliable with current global climate models [*Zhang and Walsh*, 2006; *Eisenman et al.*, 2007].

Viewed from the perspective of ice extent (Fig. 1E), September 2007 falls 4.7 detrended standard deviations below the polynomial trend (black line), and August-September-October 2007 are the three months with largest absolute deviations from this trend. The next two largest deviations are the negative anomaly in September 2008 and the positive anomaly in September 1996, which have absolute deviations that are 70% and 59% as large as September 2007, respectively. When ice edge latitude is instead considered (Fig. 3E), September 2007 is 3.2 detrended standard deviations below the polynomial trend, with August 1985 having larger absolute deviation and both December 1984 and October 1984 having at least 90% as large absolute deviations. In total, 18 months have absolute deviations of the ice edge latitude at least 60% as large as September 2007, in

contrast to 3 months having ice extent absolute deviations at least 60% as large as September 2007.

**Approximating ice edge latitude from ice extent**

A relationship between ice extent and ice edge latitude can be derived by identifying the latitude with ocean area north of it equal to the ice extent. Although this method is not used for the results presented in this study, it facilitates a convenient approximation to quickly calculate the zonal-mean ice edge latitude from ice extent. Using a 5th order polynomial expansion of the ratio between the poleward ocean area and poleward land area as a function of latitude, the zonal mean ice edge latitude for ice extents up to $16 \times 10^6$ km$^2$ can be approximately expressed as $\sin^{-1}\{1-\epsilon/[2\pi(1+1.56\epsilon-60.4\epsilon^2+458\epsilon^3-1367\epsilon^4+1389\epsilon^5)]\}$, where $\epsilon$ is the ice extent divided by the square of the radius of the earth, and $\sin^{-1}[1-\epsilon/(2\pi 0.49)]$ for larger ice extents up to $22\times10^6$ km$^2$. Applying this relationship to monthly mean sea ice extents reported by the NSIDC (http://nsidc.org/data/seaice_index/archives/) gives results (not shown) that are qualitatively equivalent to Fig. 3.

## References

Eisenman, I., N. Untersteiner, and J.S. Wettlaufer (2007), On the reliability of simulated Arctic sea ice in global climate models, *Geophys. Res. Lett.*, *34*, L10501, doi:10.1029/2007GL029914.

Shao, J. (1993), Linear-model selection by cross-validation, *J. Am. Stat. Assoc.*, *88*(422), 486–494.

Walsh, J.E. (1995), Long-term observations for monitoring of the cryosphere, *Clim. Change*, *31*(2-4), 369–394.

Weisberg, S. (2005), *Applied Linear Regression*, 3rd ed, Wiley.

Zhang, X.D., and J.E. Walsh (2006), Toward a seasonally ice-covered Arctic Ocean: Scenarios from the IPCC AR4 model simulations, *J. Clim.*, *19*(9), 1730–1747.